Title

Luminescence complementation assay for measurement of binding to protein C-termini in live cells.

Authors

Nadel, Cory M
Ran, Xu
Gestwicki, Jason E

Publication Date

2020-12-01

DOI

10.1016/j.ab.2020.113947

Peer reviewed

HHS Public Access

Author manuscript

Anal Biochem. Author manuscript; available in PMC 2021 December 15.

Published in final edited form as:

Anal Biochem. 2020 December 15; 611: 113947. doi:10.1016/j.ab.2020.113947.

Luminescence Complementation Assay for Measurement of Binding to Protein C-Termini in Live Cells

Cory M. Nadel, **Xu Ran**, **Jason E. Gestwicki***

Department of Pharmaceutical Chemistry and the Institute for Neurodegenerative Disease, University of California San Francisco, San Francisco, CA 94158

Abstract

Protein-protein interactions (PPIs) involving the extreme C-terminus serve important scaffolding and regulatory functions. Here, we leveraged NanoBiT technology to build a luminescent complementation assay for use in studying this subcategory of PPI. As a model system, we fused one component of NanoBiT to the disordered C-terminus of heat shock protein (Hsp70) and the other to its binding partner, the tetratricopeptide repeat (TPR) domain of CHIP/STUB1. We found that HEK293 cells that stably express these chimeras under a doxycycline promoter produced a robust luminescence signal. This signal was sensitive to mutations and it was further tuned by the expression of competitive C-termini. Using this system, we identified a promising, membrane permeable inhibitor of the Hsp70-CHIP interaction. More broadly, we anticipate that NanoBiT is well-suited for studying PPIs that involve C-termini.

Graphical abstract

*to whom correspondence can be addressed, Jason E. Gestwicki, UCSF, 675 Nelson Rising Lane, San Francisco, CA 94158.

AUTHOR CONTRIBUTIONS

Cory M. Nadel: Conceptualization, Methodology, Investigation, Formal Analysis, Writing-Original draft preparation. **Xu Ran:** Investigation. **Jason E. Gestwicki:** Conceptualization, Supervision, Funding acquisition, Writing – Reviewing and Editing.

DECLARATION OF COMPETING INTERESTS

The authors declare no competing financial interests.

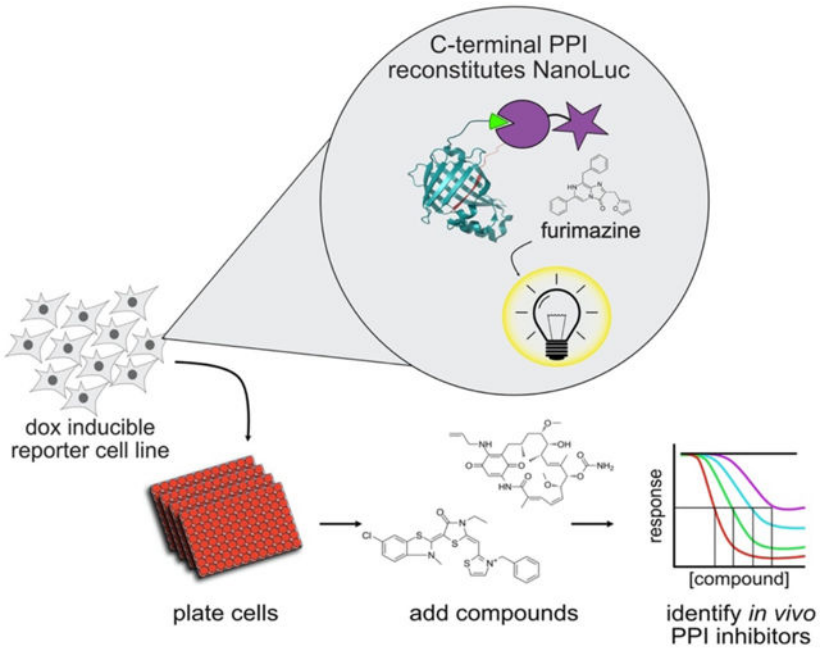

INTRODUCTION

Protein-protein interactions (PPIs) are targets for diverse diseases, including cancers and neurological disorders [1, 2]). While some progress has been made in finding PPI inhibitors, development has been relatively slow. One reason is that PPI interfaces are structurally heterogeneous; for example, they differ widely in buried surface area and apparent affinity [3]. Moreover, some PPIs involve primarily alpha helices, while others are composed of beta strands or coiled coils [4–6]. Thus, certain types of inhibitors, such as helical peptidomimetics, might be particularly well-suited for one category of PPI, but not others [7, 8]. At the same time, the assay platforms used for discovery and/or optimization of PPI inhibitors tend to be equally diverse, with fluorescence polarization (FP), AlphaScreen, NMR, surface plasmon resonance (SPR) and other technologies playing outsized roles that depend on the target (*e.g.* its affinity, size, suitability for chemical labelling) [9–12]. Thus, one important goal of the field is to develop assay technologies that are tailored towards specific sub-categories of PPIs.

One class of PPI that has been particularly under-studied involves protein termini. This type of interaction typically involves binding of the last few residues of a protein's N- or C-termini to an ordered domain of the partner protein. Multiple domains are involved in recognition of termini, including tetratricopeptide repeats (TPRs), 14–3-3 motifs and Psd95/Dig1/Zo-1 (PDZ) domains [13–15]. These domains are widespread in the proteome, linking terminal PPIs to a wide range of important biological processes [16–20]. Structurally, these interactions are usually characterized by recognition of the N-terminal amine or C-terminal carboxylate, plus nearby residues [21, 22]. For example, the TPR domain of the E3 ubiquitin ligase, CHIP/STUB1, binds to the C-terminus of heat shock protein 70 (Hsp70) via a series of cationic residues termed a "carboxylate clamp" [23]. Because protein termini are often

disordered and the major contacts are polar, this category of PPIs is quite topologically and chemically different from others [24]. However, despite their widespread importance and unique architecture, relatively few chemical inhibitors of this type of PPI are available [25–27] and few assays [28] have been specifically developed to study them, especially in cells.

Here, we describe a live-cell bimolecular luminescence complementation assay for studying C-terminal binding interactions. As a model system, we fused the disordered, C-terminal motif of Hsp70 to one component of NanoBiT and the TPR domain of CHIP to the other. Using cells that stably express these chimeras, we identified a key role for endogenous C-termini in tuning the strength of the PPI and then identified a promising, cell-permeable inhibitor. Given the roles of CHIP-Hsp70 complexes in protein homeostasis [29–31], we anticipate that this assay could be used to create an important, new chemical probe. More broadly, this work may provide a general template for studying terminal PPIs.

RESULTS

Optimization of a live-cell bimolecular luminescence complementation assay to study the CHIP-Hsp70 C-terminal interaction.

To build an assay system for studying interactions between C-terminal peptide motifs and C-terminal binding protein, we chose to leverage the NanoBiT bimolecular luminescence complementation system (Promega). Briefly, the NanoBiT platform uses an engineered split-luciferase system to detect PPIs and it has numerous features that are beneficial to this type of screening, including low background, reversibility, and the ability to be used in living cells [32]. This type of assay is created by genetically fusing proteins-of-interest to the two split components of Nano-luciferase (NanoLuc), individually termed LgBiT and SmBiT. These chimeric species are then expressed in cells at equimolar concentrations and interactions between them are detected by addition of a cell permeable furimazine substrate that is converted to light by the reconstituted NanoLuc. As the NanoBiT components have negligible affinity for one another (~190 μM), their association and the subsequent reconstitution of functional NanoLuc are dependent on the PPI being studied (Figure 1A).

As a model system, we chose to study the interaction of CHIP with the IEEVD motif that is found at the extreme C-terminus of heat shock protein (Hsp70) [33, 34]. Briefly, Hsp70 is a molecular chaperone that uses its IEEVD motif to bind the TPR domain of CHIP with an affinity of ~600 nM [35]. Because CHIP is an E3 ubiquitin ligase, this PPI is thought to facilitate degradation of Hsp70-bound, misfolded proteins [36]. To reconstitute this PPI in cells, we fused the IEEVD peptide motif to the C-terminus of LgBiT separated by a flexible GGSG linker (Figure 1B). Recent work has shown that the interaction of CHIP with the IEEVD sequence is sub-optimal and that LWWPD is preferred [21]. Indeed, LWWPD peptide bound to CHIP's purified TPR domain at least 10-fold better than IEEVD (Figure 1C), as determined by FP [21]. Therefore, to test whether the NanoBiT platform in cells was able to recapitulate this difference in affinity, we also generated a LgBiT construct fused to LWWPD. To create the other binding partner, SmBiT was fused to the N-terminus of CHIP separated by a flexible GGSG linker. Here, we created constructs with either wild type TPR domain or a variant bearing an inactivating mutation (CHIP K30A) that removes one of the carboxylate clamp residues [37]. In both cases, SmBiT was appended to the N-terminus of

the TPR, as this position was anticipated to best orient SmBiT and LgBiT during complementation.

As an initial test, these constructs were transiently transfected into HEK293T cells, and luminescence measured at 24 hours. As expected, low signal was observed in the absence of a PPI pair (Figure 1D). However, expression of the wild type NanoBiT components resulted in a 180 ± 20-fold increase in luminescence. Moreover, co-expression of the tighter affinity, LgBiT-LWWPD with SmBiT-CHIP showed greater luminescence than the LgBIT-IEEVD (300 ± 2.7-fold). Likewise, replacing SmBiT-CHIP with the mutant, SmBiT-CHIP K30A, decreased luminescence (97 ± 3.5-fold). Then, we tested whether the luminescent signal was dependent on the ratio of SmBiT:LgBiT constructs. Specifically, HEK293T were transfected with SmBiT-CHIP:LgBiT-IEEVD at ratios of 1:1, 2:1, or 1:2, while maintaining equal total volumes of DNA. After 24 hours, we found that the SmBiT:LgBiT ratio did not significantly impact the total luminescence (values ranged from ~160 to ~180; Figure 1E). Together, these results suggested that the NanoBiT platform could accurately recapitulate *in vitro* affinities and that background was low.

Generation and characterization of a doxycycline-inducible, stable reporter cell line.

To make this system more suitable for high throughput, we generated a stable cell line. Specifically, Flp-In HEK293T cells bearing a single Flp-recombinase integration site within a safe-harbor locus were co-electroporated with vectors expressing Flp recombinase and the integrating sequences (Figure 2A). Here, we used a CMV promoter-driven DNA construct that encodes both components of the NanoBiT reporter from a single transcript, separated by an Internal Ribosomal Entry Site (IRES) (Figure 2B). To facilitate identification of the individual components by western blot, we also appended an N-terminal myc-tag to LgBiT-IEEVD and a C-terminal FLAG-tag to SmBiT-CHIP. To gain temporal control, we encoded two repeats of the tetracycline operator such that the reporter is doxycycline (dox) inducible. Following recovery after transfection, cells were selected with hygromycin and single colonies derived. To characterize this stable cell line, NanoBiT cells were seeded in 96-well plates with or without dox and luminescence was assayed after 24 hours (Figure 2C). Treatment with dox increased luminescence 31-fold compared to control (47300 ± 1270 RLU, 1520 ± 490 RLU, respectively). In addition, lysates from these cells were analyzed by western blot, confirming that both reporter components were expressed in response to dox, with little background (Figure 2D). To test whether this signal is stable over time, we assayed luminescence following dox withdrawal, showing that the it was stable for at least 6 hours (Figure 2E).

The abundance and activity of a chaperone competitor tune the NanoBiT reporter signal.

The Hsp70 and Hsp90 molecular chaperones are ubiquitously expressed and highly abundant [38]. This is important because any chemical inhibitor of the Hsp70-CHIP interaction would need to contend with the abundance of these native competitors. Thus, we envisioned that one of the first uses of the NanoBiT system could be to define the roles of endogenous Hsp70 C-termini. First, we performed reciprocal co-immunoprecipitation experiments using antibodies specific for the myc- or FLAG-tags. As expected, SmBiT-CHIP-FLAG co-eluted with myc-LgBiT-IEEVD when we immunoprecipitated via the myc-

tag (Figure 3A). However, we were unable to detect myc-LgBiT-IEEVD coeluted by immunoprecipitation of SmBiT-CHIP-FLAG. This result is consistent with a competitive equilibrium with native interacting partners, such as Hsp70 (Figure 3B). Indeed, when we probed the immunoprecipitations for native Hsp70, we clearly detected coelution with SmBiT-CHIP-FLAG. To further test this contribution from endogenous Hsp70, we treated NanoBiT-expressing cells with an inhibitor of Hsp70 ATPase activity, JG-98. Hsp70 ATPase inhibitors have been shown to enhance Hsp70 client degradation via CHIP [39, 40], so we thought that treatment with JG-98 might promote competition for the NanoBiT reporter signal. Indeed, JG-98 (5 μM), but not an inactive control, JG-258, reduced luminescence (Figure 3C). To test whether these activities were dose dependent in the expected concentration, we treated with either JG-98 or JG-258 at a series of concentrations. JG-98 had an IC_{50} of 2.9 ± 0.6 μM (Figure 3D, consistent with its potency in other cells [41]. As another test of this idea, we treated the cells with an inhibitor of Hsp90, 17-DMAG, which is known to elevate Hsp70 expression levels [42]. As expected, treatment with 17-DMAG (5 μM) also reduced the luminescence (Figure 3C), presumably by elevating the levels of the competitor (see below). Treating cells with varying concentrations of 17-DMAG showed dose dependence with the expected IC_{50} of 3.1 ± 1.5 nM (Figure 3D). To independently confirm the effects of these treatments on the PPIs, we performed co-immunoprecipitation experiments. As expected, 17-DMAG increased the total abundance of Hsp70 in the lysate, compared to vehicle, resulting in increased association of SmBiT-CHIP-FLAG with Hsp70 and decreased association with myc-LgBiT-IEEVD (Figure 3E). Interestingly, we found that JG-98 treatment partially destabilized both components of the NanoBiT reporter. Despite this effect, it was still clear that JG-98 decreased association of the NanoBiT components, consistent with the luminescence measurements. Thus, the levels of endogenous C-termini, especially Hsp70, compete for binding to CHIP in the NanoBiT reporter, making the system sensitive to whether putative inhibitors can out-compete the abundant, native C-termini.

Identification of a cell-active PPI inhibitor.

There are very few inhibitors of the PPIs between proteins and C-termini [26, 43]. One of the problems with these interactions is that potential inhibitors need to mimic the negative charge of the carboxy terminus, which is expected to create difficulties in membrane permeability. As a critical test of the NanoBiT reporter, we synthesized potential inhibitors in which LWWPD was fused to cell-penetrating peptides (CPPs). To understand which CPP might perform best in this assay, we created inhibitors that employed either polyarginine (R9), penetratin (Pene), or the HIV Tat sequence (Tat) (Figure 4A). As key controls, we also included an N-terminally acetylated LWWPD peptide without a CPP and an inverted sequence, fused to Tat (termed r-Tat). Then, the NanoBiT-expressing cells were incubated with each peptide at a single concentration (10 μM) for 1 hour prior to measuring luminescence (Figure 4B). As expected, neither of the two negative controls were able to alter luminescence. Likewise, the Pen-LWWPD and Tat-LWWPD peptides were not effective, suggesting low permeability. However, the R9-LWWPD peptide reduced luminescence by approximately 40%. We subsequently performed dose response experiments and determined an IC_{50} of 2.6 ± 0.83 μM (Figure 4C). Finally, to explore the kinetics of this inhibitory effect, we treated with R9-LWWPD and measured luminescence over time (Figure 4D). In these experiments, cells were preincubated with furimazine

substrate for 30 minutes to allow luminescence to stabilize before treatment with R9-LWWPD or a DMSO control. We observed dose-dependent decreases in luminescence, which was largely complete by 8 to 10 minutes after treatment. Taken together, these results demonstrate that the NanoBiT reporter can be used to identify a cell active inhibitor of the Hsp70-CHIP interaction.

DISCUSSION

The CHIP-Hsp70 complex plays a critical role in proteostasis, mediating ubiquitination and subsequent degradation of steroid hormone receptors, ion channels and other proteins [44–46]. Accordingly, this PPI has been implicated as a potential drug target for multiple diseases, such as cystic fibrosis, where it plays roles in premature degradation of mutated CFTR [47–49]. However, while chemical inhibitors of the CHIP-Hsp70 interaction hold promise [25, 26, 50, 51], this target has been difficult, likely owing to its polar nature and the high concentration of endogenous C-termini. To accelerate this field, we developed a NanoBiT reporter that appears suitable for studying this important PPI. Importantly, we found that NanoBiT accurately recapitulated *in vitro* binding affinities (see Figure 1). Hsp70's interactions with TPR co-chaperones are relatively weak (~1 to 5 μM; [35]), making them relatively difficult to study with conventional, cellular PPI assays. NanoBiT, however, was sensitive enough to detect the CHIP-Hsp70 PPI, as well as discern changes in binding strength due to mutations of CHIP or optimization of the C-terminal peptide motif. This sensitivity likely arises from the exceptionally low background binding of LgBiT and SmBiT (K_d ~ 190 μM). Using this assay, we also defined a clear role for endogenous competitors in dampening the NanoBiT reporter activity (see Figure 3). This feature is expected to be critical, and difficult to replicate *in vitro*, as any successful therapeutic would need to contend with this competitor pool. Finally, inhibitor efficacy in this NanoBiT assay requires membrane permeability. While this is always an important property, it is particularly challenging for C-terminal PPIs because of the dominance of polar contacts. Indeed, we found that Ac-LWWPD had no efficacy in the NanoBiT assay (despite its sub-micromolar affinity *in vitro;* see Figure 1), and required fusion to a CPP (see Figure 4). Together, we anticipate that the features of this NanoBiT assay are well-suited for development of inhibitors for the CHIP-Hsp70 interaction. More broadly, the development of terminal PPI inhibitors has lagged behind those targeting other interfaces. While the unique physicochemical aspects of protein termini (*e.g.* disorder, charge, post-translational modifications, etc.) are an impedance, we anticipate that variants of this NanoBiT assay could be used to study other N- and C-terminal contacts.

METHODS

Reagents and General Methods

Antibodies used in this study: mouse anti-c-myc clone 9E10 (Invitrogen, lot #TL276981), rabbit anti-DYKDDDDK tag clone D6W5B (Cell Signaling Technologies, lot #5), rabbit anti-Hsp70/Hsc70 clone H-300 (Santa Cruz Biotechnology, lot #D1913), mouse anti-alpha tubulin (Cell Signaling Technologies, lot #15), secondary anti-rabbit IRDye 680RD (Licor, lot #C90827–25), secondary anti-mouse IRDye 800CW (Licor, lot #C90806–05). Reagents

used for co-immunoprecipitation: Pierce anti-c-myc magnetic beads (Thermo Fisher, lot #UD283468), anti-FLAG M2 magnetic beads (Sigma, lot #SLCD8977). Gibco cell culture reagents (media, fetal bovine serum, 10X penicillin/streptomycin, 0.05% trypsin-EDTA) were purchased from Invitrogen. Other inhibitors and antibiotics: JG-98 (synthesized as previously described [52]), 17-DMAG (Cayman Chemical), zeocin (Invitrogen), blasticidin (Invitrogen), and doxycycline (CalBiochem). Restriction enzymes were purchased from New England BioLabs. Data analysis and curve fitting was performed using GraphPad Prism 8.

Plasmids

PCR primers (purchased from Integrated DNA Technologies) and plasmids used in this study are provided in Tables S1 and S2 below, respectively. For NanoBiT transfection experiments, PCR was used to append C-terminal sequences onto LgBiT and to isolate coding sequences for WT or K30A CHIP. LgBiT C-terminal sequences were inserted into pBiT1.1-N[TK/LgBiT] digested with HindIII/XhoI by Gibson assembly as previously described [53]. Likewise, Gibson assembly was used to insert CHIP WT or K30A sequences into pBiT2.1-N[TK/SmBiT] digested with XhoI/SacI. To construct the bicistronic vector for generation of a stable NanoBiT cell line, myc-LgBiT-IEEVD, SmBiT-CHIP-FLAG, and IRES2 sequences were first isolated by PCR with overlapping regions. Overlap extension PCR was used to combine these into a single double-stranded DNA sequence which was subsequently inserted into pcDNA3-FRT-TO digested with KpnI/XhoI by Gibson assembly. All DNA constructs used in this study were confirmed by sequencing (Elim Biopharm).

Peptide Synthesis

CHIP inhibitor peptides were synthesized using microwave-assisted, solid-phase peptide synthesis in an Fmoc protecting group strategy as previously described [55]. Synthesized peptides were cleaved in 87.5% trifluoroacetic acid (TFA), 5% dithiothreitol (DTT), 5% water and 2.5% triisopropylsilane, precipitated with ethyl ether and purified with reverse phase, semi-preparative HPLC. Peptide purities were determined to be >90% by HPLC. Peptides were stored as dry powders at −80 °C and dissolved in DMSO prior to use.

Tissue Culture

HEK 293T cells (ATCC) were cultured in Dulbecco's Modified Eagle Medium (DMEM) supplemented with 10% Fetal Bovine Serum (FBS) and penicillin/streptomycin and maintained at 37 °C / 5% CO_2 in a humidified incubator. For transfections, cells were plated in poly-D-lysine coated white, clear-bottom 96-well plates and cultured overnight. 1 hour prior to transfection, media was changed to Opti-Mem reduced serum media to induce serum starvation. Transfection complexes were created by mixing 50 ng of each SmBiT/LgBiT plasmid DNA (100 ng total DNA per well) with Lipofectamine 2000 (Thermo Fisher) at DNA:lipid ratio of 1 μg:2.5 μL in Opti-Mem. Complexes were incubated at room temperature for 30 minutes, then applied dropwise to cells. Cells were transfected for 6 hours; following, transfection complexes were removed, and media was changed to 10% FBS-DMEM. Cells were placed back in the incubator overnight prior to analysis.

For construction of the stable NanoBiT reporter cell line, parental HEK 293 Flp-In T-REx cells (Thermo Fisher) were cultured in 10% FBS-DMEM supplemented with 1X penicillin/streptomycin, 15 μg/mL blasticidin, and 100 μg/mL zeocin. Cells were harvested by trypsinization, resuspended in electroporation buffer containing 5 μg NanoBiT bicistronic vector DNA and 45 μg pOG44 plasmid DNA. Cells were electroporated using program Q-001 on a Lonza 4D-Nucleofector. Electroporated cells were immediately diluted in 10% FBS-DMEM and cultured for 48 hours to recover. Following recovery, cells were selected with 100 μg/mL hygromycin until single colonies arose. Colonies were subsequently picked and screened for dox-inducible expression of reporter components and luminescence.

Luminescence Assays

Luminescence recordings were performed on live cells plated in poly-D-lysine coated white 96-well plates. Nano-Glo Live Cell Substrate (Promega) was prepared by diluting 1 volume of Nano-Glo Live Cell Reagent into 19 volumes of Nano-Glo LCS Buffer (12.5 μL per well), and then added to fresh Opti-Mem media (50 μL per well). To record luminescence, media was removed from cells and 62.5 μL of prepared substrate in media was added to each well. Luminescence was allowed to stabilize by placing plates in the dark for 5 minutes at room temperature. Luminescence was then measured on a SpectraMax M5 plate reader with 500 ms integration time. Untransfected or uninduced reporter cells were used to obtain background measurements which were subtracted from observed luminescence values. Where applicable, luminescence values were normalized to DMSO controls and presented as percent of total.

Cell lysis and co-immunoprecipitation

NanoBiT HEK293 cells were harvested by trypsinization, resuspended in media containing doxycycline to induce reporter expression, and cultured overnight. Following, cells were washed once in 1X Dulbecco's Phosphate Buffered Saline and lysed in 1 mL ice cold non-denaturing lysis buffer (25 mM Tris-HCl pH 7.4, 150 mM NaCl, 1 mM EDTA, 1% NP-40). Lysates were collected by gentle scraping, transferred to 1.7 mL microcentrifuge tubes, and incubated on ice for 15 minutes. Following, samples were subjected to centrifugation at 15000 RPM for 10 minutes at 4 °C and supernatants were transferred to new microcentrifuge tubes. Relative protein concentrations were determined by bicinchoninic acid assay (Pierce) and samples were normalized to the lowest protein concentration.

For immunoprecipitation, a representative input sample of 40 μL was collected, mixed with 20 μL 3X SDS-PAGE loading buffer (188 mM Tris-HCl pH 6.8, 3% SDS, 30% glycerol, 0.01% bromophenol blue, 15% β-mercaptoethanol), denatured at 95 °C for 5 minutes, and stored at 4 °C for later analysis. 30 μL magnetic beads per condition were collected and washed twice in ice cold, non-denaturing lysis buffer. Beads were resuspended in 30 μL non-denaturing lysis buffer per condition and added to prepared lysates. Samples were incubated at 4 °C overnight with rotation. The following day, beads were collected by magnet and supernatants were removed. Beads were washed 3 times in ice cold, non-denaturing lysis buffer, and bound proteins were eluted by addition of 60 μL 2X SDS-PAGE loading buffer and denaturing at 95 °C for 5 minutes. Inputs and eluates were subsequently analyzed by SDS-PAGE followed by western blotting.

Western Blotting

Prepared lysates were separated on precast 4–20% SDS-PAGE gradient gels (Bio-Rad) for 35 minutes at 200V. Proteins were transferred to nitrocellulose membranes using a Trans-Blot Turbo Transfer System (Bio-Rad). Membranes were blocked in Odyssey PBS Blocking Buffer (Licor) for 1 hour at room temperature and then incubated in primary antibody diluted 1:1000 in Odyssey PBS Blocking Buffer overnight at 4 °C. The following day, membranes were washed 3 times in 1X Tris-Buffered Saline containing 0.05% Tween-20 (TBS-T) and then incubated in secondary antibody diluted 1:10000 in Odyssey PBS Blocking Buffer for one hour at room temperature. Following incubation with secondary antibody, membranes were washed 3 times in 1X TBS-T and imaged on an Odyssey Fc Imaging System (Licor).

Supplementary Material

Refer to Web version on PubMed Central for supplementary material.

ACKNOWLEDGEMENTS

The authors thank Matthew Ravalin for helpful advice and reagents. This work was supported by a grant from the NIH (NS059690).

LITERATURE CITED

1. Arkin MR and Whitty A, The road less traveled: modulating signal transduction enzymes by inhibiting their protein-protein interactions. Curr Opin Chem Biol, 2009. 13(3): p. 284–90. [PubMed: 19553156]
2. Zhong M, et al., Modulating protein-protein interaction networks in protein homeostasis. Curr Opin Chem Biol, 2019. 50: p. 55–65. [PubMed: 30913483]
3. Cesa LC, Mapp AK, and Gestwicki JE, Direct and Propagated Effects of Small Molecules on Protein-Protein Interaction Networks. Front Bioeng Biotechnol, 2015. 3: p. 119. [PubMed: 26380257]
4. Watkins AM and Arora PS, Anatomy of beta-strands at protein-protein interfaces. ACS Chem Biol, 2014. 9(8): p. 1747–54. [PubMed: 24870802]
5. Watkins AM, Wuo MG, and Arora PS, Protein-Protein Interactions Mediated by Helical Tertiary Structure Motifs. J Am Chem Soc, 2015. 137(36): p. 11622–30.
6. Wuo MG, Mahon AB, and Arora PS, An Effective Strategy for Stabilizing Minimal Coiled Coil Mimetics. J Am Chem Soc, 2015. 137(36): p. 11618–21.
7. Ran X and Gestwicki JE, Inhibitors of protein-protein interactions (PPIs): an analysis of scaffold choices and buried surface area. Curr Opin Chem Biol, 2018. 44: p. 75–86. [PubMed: 29908451]
8. Botta J, et al., Design and development of stapled transmembrane peptides that disrupt the activity of G-protein-coupled receptor oligomers. J Biol Chem, 2019. 294(45): p. 16587–16603.
9. Bower JF and Pannifer A, Using fragment-based technologies to target protein-protein interactions. Curr Pharm Des, 2012. 18(30): p. 4685–96. [PubMed: 22650253]
10. Choulier L, et al., Chemical library screening using a SPR-based inhibition in solution assay: simulations and experimental validation. Anal Chem, 2013. 85(18): p. 8787–95. [PubMed: 23931734]
11. Yasgar A, et al., AlphaScreen-Based Assays: Ultra-High-Throughput Screening for Small-Molecule Inhibitors of Challenging Enzymes and Protein-Protein Interactions. Methods Mol Biol, 2016. 1439: p. 77–98. [PubMed: 27316989]

12. Nikolovska-Coleska Z, et al., Development and optimization of a binding assay for the XIAP BIR3 domain using fluorescence polarization. Anal Biochem, 2004. 332(2): p. 261–73. [PubMed: 15325294]
13. Scheufler C, et al., Structure of TPR domain-peptide complexes: critical elements in the assembly of the Hsp70-Hsp90 multichaperone machine. Cell, 2000. 101(2): p. 199–210. [PubMed: 10786835]
14. Das AK, Cohen PW, and Barford D, The structure of the tetratricopeptide repeats of protein phosphatase 5: implications for TPR-mediated protein-protein interactions. EMBO J, 1998. 17(5): p. 1192–9. [PubMed: 9482716]
15. Hillier BJ, et al., Unexpected modes of PDZ domain scaffolding revealed by structure of nNOS-syntrophin complex. Science, 1999. 284(5415): p. 812–5. [PubMed: 10221915]
16. Koren I, et al., The Eukaryotic Proteome Is Shaped by E3 Ubiquitin Ligases Targeting C-Terminal Degrons. Cell, 2018. 173(7): p. 1622–1635 e14.
17. Varshavsky A, N-degron and C-degron pathways of protein degradation. Proc Natl Acad Sci U S A, 2019. 116(2): p. 358–366. [PubMed: 30622213]
18. Ravalin M, et al., End-Binding E3 Ubiquitin Ligases Enable Protease Signaling. ACS Chem Biol, 2019.
19. Christopherson KS, et al., PSD-95 assembles a ternary complex with the N-methyl-D-aspartic acid receptor and a bivalent neuronal NO synthase PDZ domain. J Biol Chem, 1999. 274(39): p. 27467–73.
20. Schumacher B, et al., Structure of the p53 C-terminus bound to 14–3-3: implications for stabilization of the p53 tetramer. FEBS Lett, 2010. 584(8): p. 1443–8. [PubMed: 20206173]
21. Ravalin M, et al., Specificity for latent C termini links the E3 ubiquitin ligase CHIP to caspases. Nat Chem Biol, 2019. 15(8): p. 786–794. [PubMed: 31320752]
22. Wilson CG, Kajander T, and Regan L, The crystal structure of NlpI. A prokaryotic tetratricopeptide repeat protein with a globular fold. FEBS J, 2005. 272(1): p. 166–79. [PubMed: 15634341]
23. Prasad BD, Goel S, and Krishna P, In silico identification of carboxylate clamp type tetratricopeptide repeat proteins in Arabidopsis and rice as putative co-chaperones of Hsp90/Hsp70. PLoS One, 2010. 5(9): p. e12761.
24. Harris BZ, et al., Role of electrostatic interactions in PDZ domain ligand recognition. Biochemistry, 2003. 42(10): p. 2797–805. [PubMed: 12627945]
25. Ardi VC, et al., Macrocycles that inhibit the binding between heat shock protein 90 and TPR-containing proteins. ACS Chem Biol, 2011. 6(12): p. 1357–66. [PubMed: 21950602]
26. Rahimi MN and McAlpine SR, Protein-protein inhibitor designed de novo to target the MEEVD region on the C-terminus of Hsp90 and block co-chaperone activity. Chem Commun (Camb), 2019. 55(6): p. 846–849. [PubMed: 30575826]
27. Stevers LM, et al., Modulators of 14–3-3 Protein-Protein Interactions. J Med Chem, 2018. 61(9): p. 3755–3778. [PubMed: 28968506]
28. Ichikawa DM, et al., A Multireporter Bacterial 2-Hybrid Assay for the High-Throughput and Dynamic Assay of PDZ Domain-Peptide Interactions. ACS Synth Biol, 2019. 8(5): p. 918–928. [PubMed: 30969105]
29. Jinwal UK, et al., Imbalance of Hsp70 family variants fosters tau accumulation. FASEB J, 2013. 27(4): p. 1450–9. [PubMed: 23271055]
30. Liu C, et al., Proteostasis by STUB1/HSP70 complex controls sensitivity to androgen receptor targeted therapy in advanced prostate cancer. Nat Commun, 2018. 9(1): p. 4700. [PubMed: 30446660]
31. Tawo R, et al., The Ubiquitin Ligase CHIP Integrates Proteostasis and Aging by Regulation of Insulin Receptor Turnover. Cell, 2017. 169(3): p. 470–482 e13.
32. Dixon AS, et al., NanoLuc Complementation Reporter Optimized for Accurate Measurement of Protein Interactions in Cells. ACS Chem Biol, 2016. 11(2): p. 400–8. [PubMed: 26569370]
33. Ballinger CA, et al., Identification of CHIP, a novel tetratricopeptide repeat-containing protein that interacts with heat shock proteins and negatively regulates chaperone functions. Mol Cell Biol, 1999. 19(6): p. 4535–45. [PubMed: 10330192]

34. Zhang M, et al., Chaperoned ubiquitylation--crystal structures of the CHIP U box E3 ubiquitin ligase and a CHIP-Ubc13-Uev1a complex. Mol Cell, 2005. 20(4): p. 525–38. [PubMed: 16307917]
35. Assimon VA, Southworth DR, and Gestwicki JE, Specific Binding of Tetratricopeptide Repeat Proteins to Heat Shock Protein 70 (Hsp70) and Heat Shock Protein 90 (Hsp90) Is Regulated by Affinity and Phosphorylation. Biochemistry, 2015. 54(48): p. 7120–31. [PubMed: 26565746]
36. Murata S, et al., CHIP is a chaperone-dependent E3 ligase that ubiquitylates unfolded protein. EMBO Rep, 2001. 2(12): p. 1133–8. [PubMed: 11743028]
37. Qian SB, et al., Engineering a ubiquitin ligase reveals conformational flexibility required for ubiquitin transfer. J Biol Chem, 2009. 284(39): p. 26797–802.
38. Genest O, Wickner S, and Doyle SM, Hsp90 and Hsp70 chaperones: Collaborators in protein remodeling. J Biol Chem, 2019. 294(6): p. 2109–2120. [PubMed: 30401745]
39. Jinwal UK, et al., Chemical manipulation of hsp70 ATPase activity regulates tau stability. J Neurosci, 2009. 29(39): p. 12079–88.
40. Davis AK, et al., Hsp70:CHIP ubiquitinates dysfunctional but not native neuronal NO synthase. Mol Pharmacol, 2020.
41. Shao H, et al., Exploration of Benzothiazole Rhodacyanines as Allosteric Inhibitors of Protein-Protein Interactions with Heat Shock Protein 70 (Hsp70). J Med Chem, 2018. 61(14): p. 6163–6177. [PubMed: 29953808]
42. Kummar S, et al., Phase I trial of 17-dimethylaminoethylamino-17-demethoxygeldanamycin (17-DMAG), a heat shock protein inhibitor, administered twice weekly in patients with advanced malignancies. Eur J Cancer, 2010. 46(2): p. 340–7. [PubMed: 19945858]
43. Voter AF, et al., A High-Throughput Screening Strategy to Identify Inhibitors of SSB Protein-Protein Interactions in an Academic Screening Facility. SLAS Discov, 2018. 23(1): p. 94–101. [PubMed: 28570838]
44. Connell P, et al., The co-chaperone CHIP regulates protein triage decisions mediated by heat-shock proteins. Nat Cell Biol, 2001. 3(1): p. 93–6. [PubMed: 11146632]
45. Jiang J, et al., CHIP is a U-box-dependent E3 ubiquitin ligase: identification of Hsc70 as a target for ubiquitylation. J Biol Chem, 2001. 276(46): p. 42938–44.
46. Joshi V, et al., A Decade of Boon or Burden: What Has the CHIP Ever Done for Cellular Protein Quality Control Mechanism Implicated in Neurodegeneration and Aging? Front Mol Neurosci, 2016. 9: p. 93. [PubMed: 27757073]
47. Meacham GC, et al., The Hsc70 co-chaperone CHIP targets immature CFTR for proteasomal degradation. Nat Cell Biol, 2001. 3(1): p. 100–5. [PubMed: 11146634]
48. Kim Chiaw P, et al., Hsp70 and DNAJA2 limit CFTR levels through degradation. PLoS One, 2019. 14(8): p. e0220984.
49. Balch WE, Roth DM, and Hutt DM, Emergent properties of proteostasis in managing cystic fibrosis. Cold Spring Harb Perspect Biol, 2011. 3(2).
50. Kunicki JB, et al., Synthesis and evaluation of biotinylated sansalvamide A analogs and their modulation of Hsp90. Bioorg Med Chem Lett, 2011. 21(16): p. 4716–9. [PubMed: 21764310]
51. Cortajarena AL and Regan L, Ligand binding by TPR domains. Protein Sci, 2006. 15(5): p. 1193–8. [PubMed: 16641492]
52. Li X, et al., Validation of the Hsp70-Bag3 protein-protein interaction as a potential therapeutic target in cancer. Mol Cancer Ther, 2015. 14(3): p. 642–8. [PubMed: 25564440]
53. Gibson DG, et al., Enzymatic assembly of DNA molecules up to several hundred kilobases. Nat Methods, 2009. 6(5): p. 343–5. [PubMed: 19363495]
54. Rousseaux MW, et al., TRIM28 regulates the nuclear accumulation and toxicity of both alpha-synuclein and tau. Elife, 2016. 5.
55. Ran X, et al., Rational design and screening of peptide-based inhibitors of heat shock factor 1 (HSF1). Bioorg Med Chem, 2018. 26(19): p. 5299–5306. [PubMed: 29661622]

Highlights

- Binding events involving a protein's extreme C-terminus are involved in many important protein-protein interactions (PPIs).
- A live-cell NanoBiT luciferase complementation assay that reports on C-terminal PPIs was developed to study the interaction of heat shock protein 70 (Hsp70) and the E3 ubiquitin ligase CHIP.
- A cell-permeant peptide inhibitor of the Hsp70-CHIP interaction was identified.

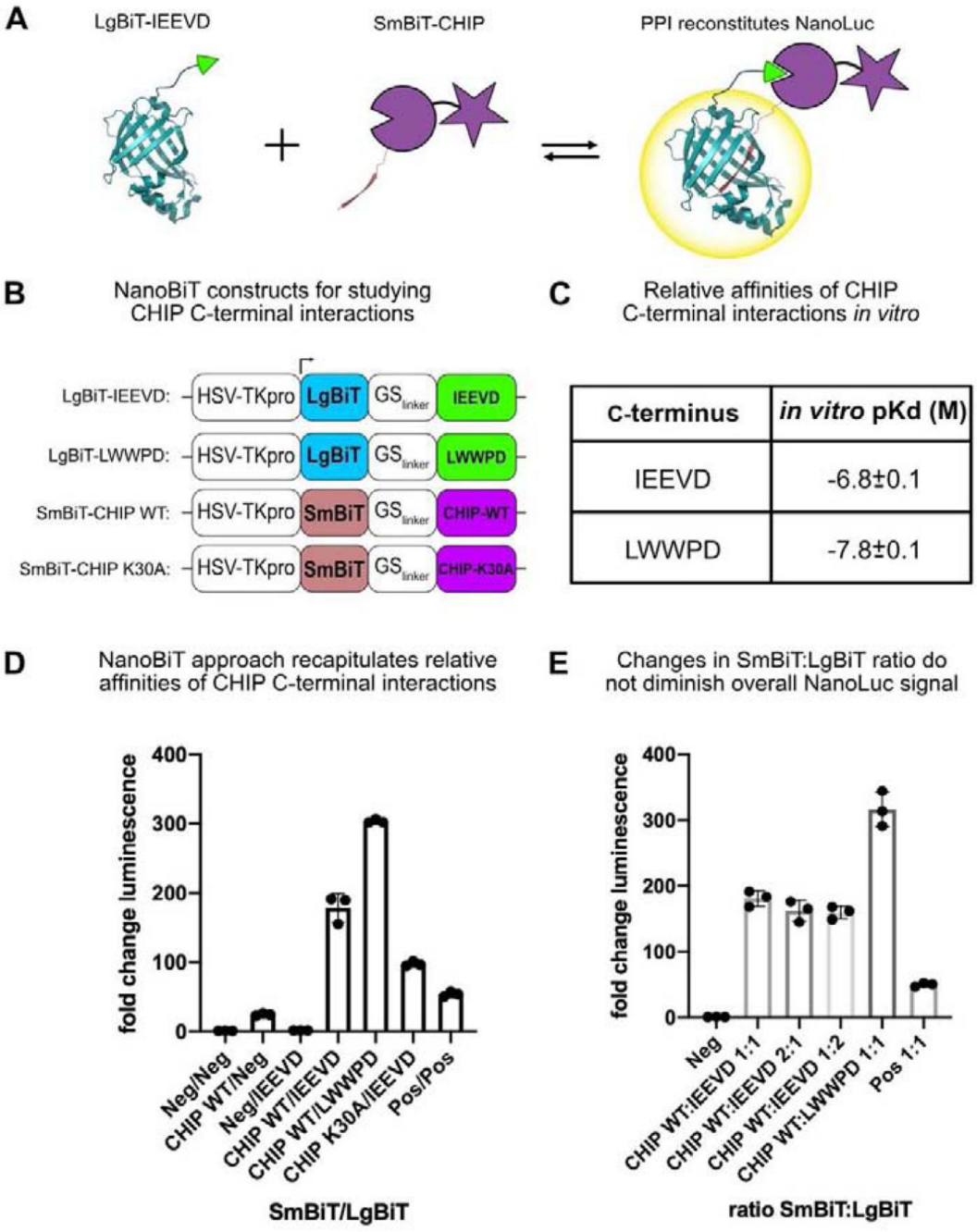

Figure 1: Optimization of a live cell platform for studying CHIP – C-terminal interactions.

(A) Schematic of the NanoBiT complementation assay for measuring CHIP binding to extreme C-termini. **(B)** DNA vectors used in this study. **(C)** Affinities of C-terminal peptides for CHIP *in vitro,* as determined by fluorescence polarization (adapted from [21]). **(D)** NanoBiT luciferase complementation assay in HEK293T cells. Cells were transfected with the denoted SmBiT and LgBiT constructs and assayed for luminescence 24 hours later. Luminescence values were normalized to the negative control and expressed as mean fold change ± SD (n=3). **(E)** Optimization of the SmBiT:LgBiT ratio. HEK293T were transfected

with the SmBiT and LgBiT constructs at the specified ratio, while maintaining equivalent total amounts of DNA. Luminescence was assayed 24 hours after transection. Values were normalized to the negative control and expressed as mean fold change ± SD (n=3).

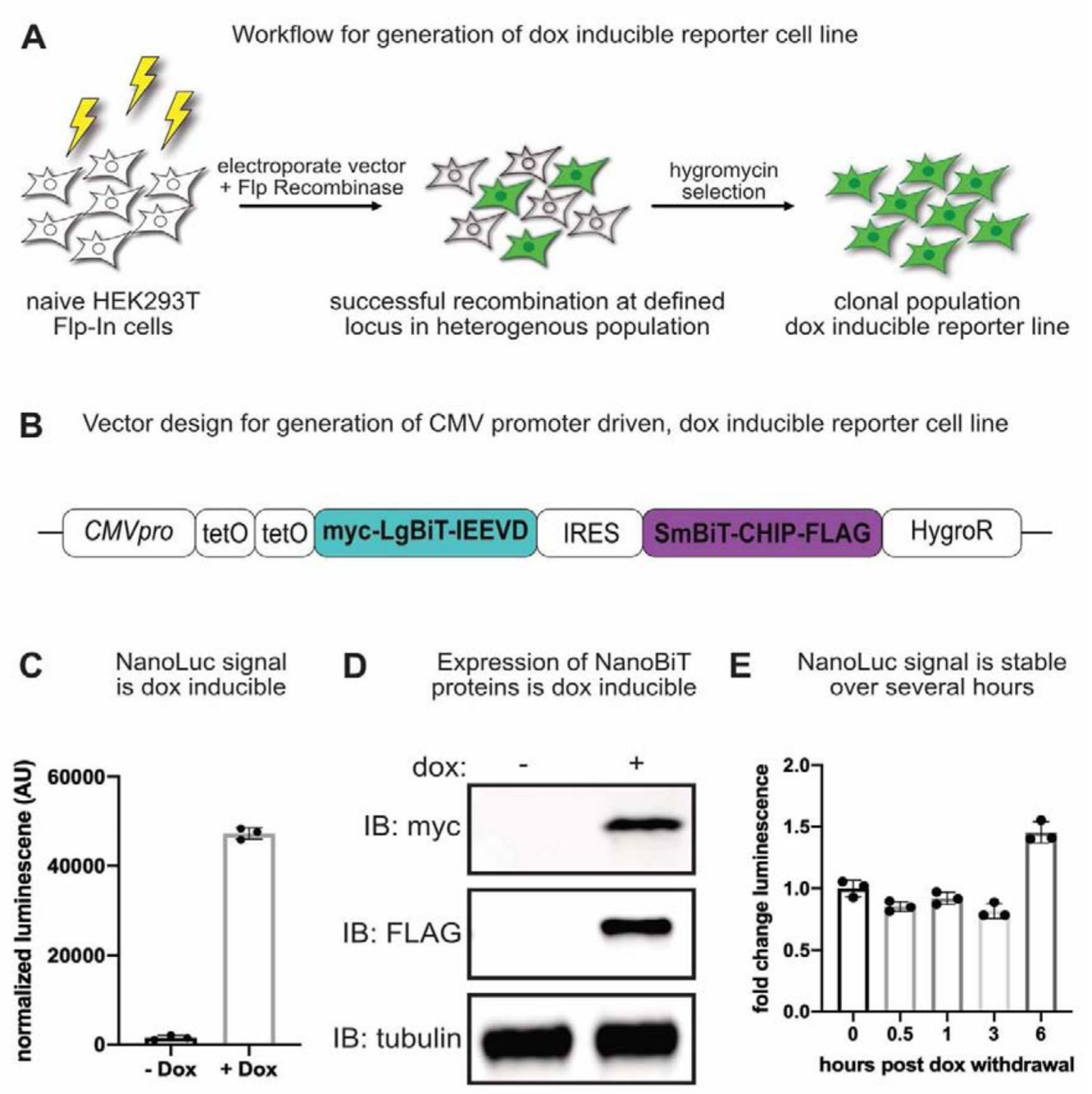

Figure 2: A stable, dox-inducible reporter cell line for studying CHIP – C-terminal interactions.

(A) Workflow for generation of a stable, clonal reporter cell line. **(B)** Architecture of the dox-inducible bicistronic vector. **(C)** NanoBiT luminescence assay showing dox-dependence of luminescence. NanoBiT cells were cultured with or without dox (100 μg/mL) and luminescence was assayed 24 hours later. Values are plotted as mean luminescence ± SD (n=3). **(D)** Western blot analysis of NanoBiT components. NanoBiT cells were cultured with or without dox (100 μg/mL) and lysates were collected 24 hours later. Probing with anti-myc or anti-FLAG shows dox-dependent induction of NanoBiT components. **(E)** NanoBiT

luminescence assay for signal stability following dox withdrawal. NanoBiT reporter was induced overnight by culturing in dox (100 μg/mL). Dox was withdrawn by addition of fresh media and luminescence was assayed at the denoted time points. Luminescence values were normalized to the 0-hour timepoint and expressed as mean fold change ± SD (n=3).

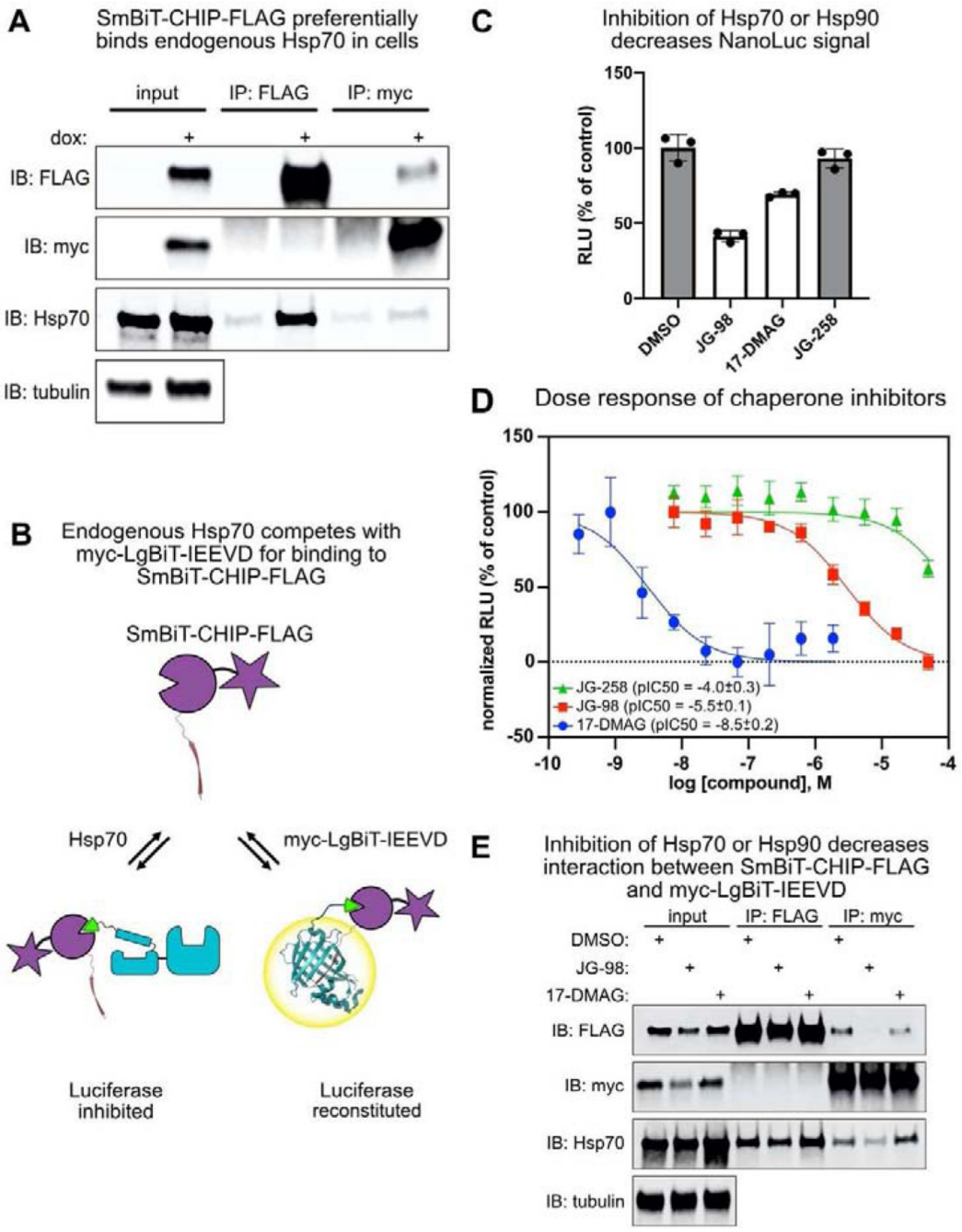

Figure 3: Endogenous C-termini tune NanoBiT reporter activity.

(A) Co-immunoprecipitation reveals competition by endogenous Hsp70. NanoBiT cells were induced by overnight incubation with dox (100 μg/mL). Endogenous Hsp70 bound to the SmBiT-CHIP-FLAG. (B) A model for competition between endogenous Hsp70 and myc-LgBiT-IEEVD. (C) Inhibitors reduce NanoBiT reporter luminescence through effects on Hsp70 function and levels. NanoBiT reporter was induced overnight and cells were treated with inhibitors (5 μM) for 6 hours. JG-98 is an Hsp70 inhibitor and JG-258 is a negative control. 17-DMAG is an Hsp90 inhibitor that induces Hsp70 levels. Luminescence

was assayed and values were normalized to the DMSO control. Values are expressed as mean percent of control ± SD (n=3). Gray bars indicate negative controls. (D) Dose response of chaperone inhibitors suggests on-target activity. NanoBiT reporter was induced overnight and cells were treated with inhibitors for 6 hours. Values were normalized to the DMSO control and expressed as mean percent of control ± SD (n=3). (E) Chaperone inhibitors block interactions between NanoBiT reporter components. Lysates from cells treated as in D were collected and reporter components immunoprecipitated on anti-FLAG or anti-myc beads.

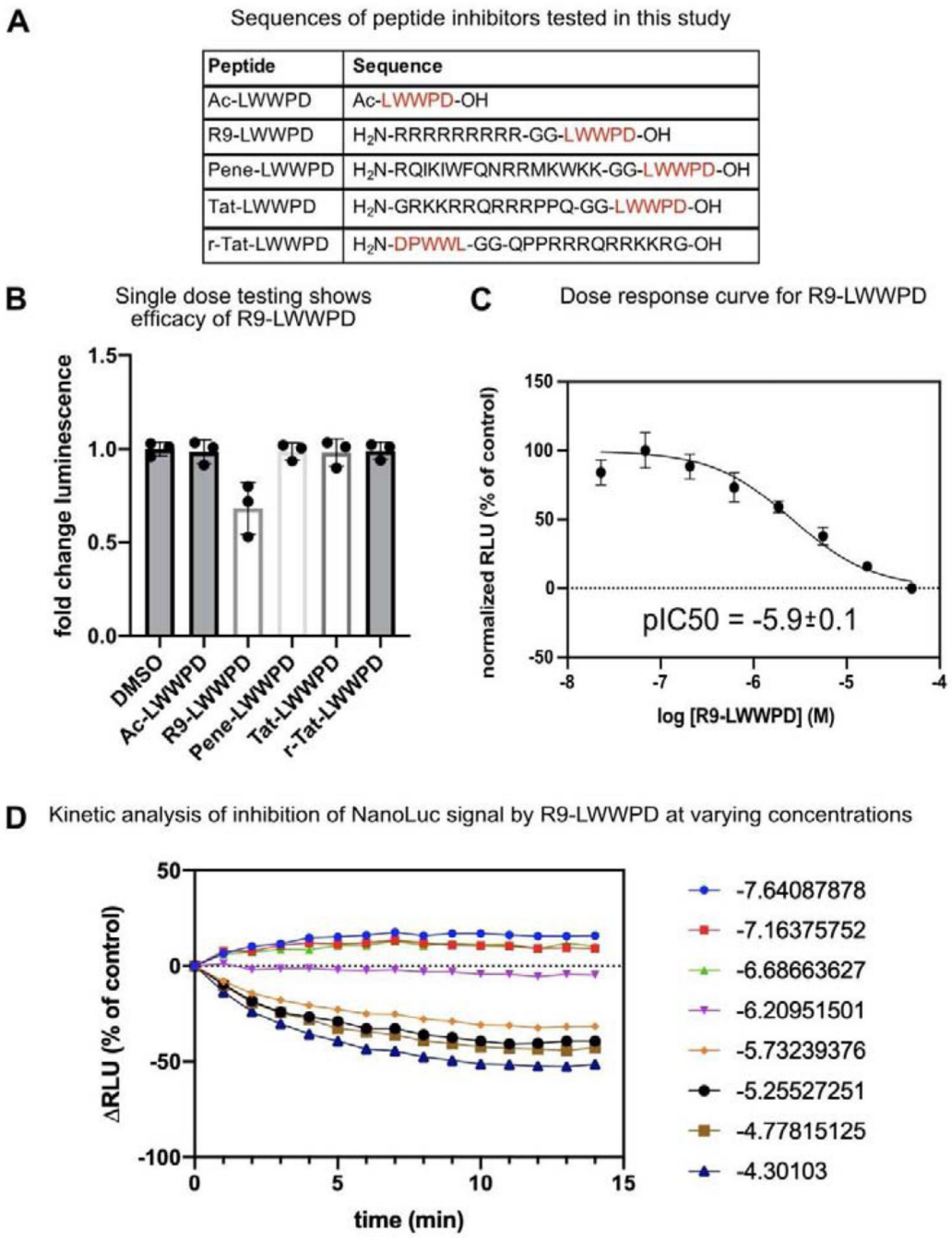

Figure 4: Identification of a cell-active inhibitor of CHIP – C-terminal PPIs.

(A) Peptide sequences of inhibitors used in this study. The CHIP-binding LWWPD region is highlighted (red). (B) Single-dose testing reveals a cell active inhibitor (R9-LWWPD). NanoBiT reporter was induced overnight and cells were treated with inhibitors (10 μM) for 1 hour. Luminescence values were normalized to DMSO control and reported as mean percent of control ± SD (n=3). Gray bars indicate negative controls. (C) Dose response of R9-LWWPD. Luminescence was measured as in B. (D) The NanoBiT reporter is rapidly responsive to inhibitors. NanoBiT cells expressing reporter were incubated in luminescence

substrate for 30 minutes to allow luminescence to stabilize. Then, cells were treated with R9-LWWPD and luminescence was measured every minute for 15 minutes. Values were normalized to DMSO control and expressed as mean change in RLU from the 0-time point (n=3). Concentrations are in log M. Error bars are omitted for clarity.